and

$$f_j(\bar{y},\bar{z}) = \phi(\bar{y},\bar{z})P_{mj}(\bar{y})P_{nj}(\bar{z}), \qquad j = 1, 2, 3, \ldots, N \quad (7)$$

where $P_{mj}(\bar{y}) = (\bar{y})^{mj}$ and $P_{nj}(\bar{z}) = (\bar{z})^{nj}$ are the same as those for isosceles triangular ducts, except that the terms with odd exponents are retained due to lack of symmetry. Detailed steps leading to the solution are in Ref. 1. The characteristic length is equal to the base a (Fig. 2).

The circumferential average and mean Nusselt numbers when $\beta = 2.5$, 5, 10, 15, 20, 25, 30, 35, 40, and 45 deg are reported in Table 3. The definitions of the Nusselt number and the Reynolds number are the same as in the previous case; however, X differs since the value of the characteristic length a is different. For instance, when $\beta = 45$ deg in right triangular ducts, $Nu = 8.169$ and $\bar{Nu} = 12.778$ at $X = 0.0004$, whereas, for an isosceles triangular duct with $2\beta = 90$ deg, $Nu = 8.284$ and $\bar{Nu} = 12.227$ at $X = 0.0008$. The difference is 1% in Nu and 4% in $\bar{Nu} = 12.227$, and this error decreases as X increases.

Equations (2) and (3) yield a relation for calculating the bulk temperature T_b. The mean Nusselt numbers in Tables 1-3 yield the values of the bulk temperature from the relation $(T_b - T_w)/(T_o - T_w) = \exp(-4\bar{Nu}Xa^2/D_e^2)$, where T_w and T_o are wall and entering fluid temperatures.

For right triangular passages, with the included angle β tending to zero, the cross sections resemble that of parallel-plate ducts. The Nusselt number data, far away from the inlet, also reflect the same trend (note D_e is different[2]). Also as $\beta \to 0$, the results for isosceles triangular ducts with angle 2β approach that of right triangular ducts with included angle β. The accuracy of the solution, especially at small X, increases as the degree of polynomials, m_j or n_j, increases. The degree of polynomials for isosceles triangular ducts is eight corresponding to $N = 25$ terms ($m_j = 7$ and $N = 20$ for $\beta < 5$ deg), whereas it is six for right triangular ducts corresponding to $N = 28$. This is because the temperature is symmetric about the y axis (see Fig. 1), and all terms containing z to the odd powers are omitted. For this reason, one may conclude that more accurate results for right triangular ducts with small included angle may be obtained from the isosceles triangular duct solution.

References

[1]Lakshminarayanan, R., and Haji-Sheikh, A., "A Generalized Closed-Form Solution to Thermal Entrance Problems," *Heat Transfer 86*, edited by C. L. Tien, V. P. Carey, and J. K. Ferrell, Hemisphere, New York, 1986, pp. 871-876.

[2]Haji-Sheikh, A., Mashena, M., and Haji-Sheikh, M. J., "Heat Transfer Coefficient in Ducts with Constant Wall Temperature," *ASME Journal of Heat Transfer*, Vol. 105, No. 4, 1983, pp. 878-883.

[3]Haji-Sheikh, A., and Beck, J. V., "Green's Function Partitioning in Galerkin-Based Integral Solution of the Diffusion Equation," *ASME Journal of Heat Transfer*, Vol. 112, No. 1, 1990, pp. 28-34.

[4]Shah, R. K., and London, A. L., "Laminar Flow Forced Convection in Ducts," Suppl. 1, *Advances in Heat Transfer*, Academic Press, New York, 1978, p. 245.

[5]Lakshminarayanan, R., "Integral Solutions to Laminar Entrance Problems in Irregular Ducts," Ph.D. Dissertation, Univ. of Texas at Arlington, Arlington, TX 1988.

Turbulent Heat Transfer in a Square Channel with Staggered Discrete Ribs

S. C. Lau,* R. T. Kukreja,† and R. D. McMillin†

Texas A&M University, College Station, Texas 77843-3123

Received June 1, 1990; revision received Sept. 20, 1990, accepted for publication Oct. 2, 1990.

*Associate Professor, Department of Mechanical Engineering.

†Graduate Student, Department of Mechanical Engineering.

Nomenclature

D	=	hydraulic diameter of square channel, [m]
dP/dx	=	streamwise pressure gradient in fully developed region, [N/m^3]
$\bar{f}$	=	friction factor, $(-dP/dx)D/\{2\dot{m}^2/(\rho D^4)\}$
$\dot{m}$	=	rate of mass flow of air, [kg/sec]
$\dot{q}_r''$, $\dot{q}_s''$	=	net heat fluxes on ribbed walls and smooth walls, [W/m^2]
Re_D	=	Reynolds number based on channel hydraulic diameter, $\dot{m}/(D\mu)$
$\overline{St}$	=	average Stanton number, the average of St_r and St_s
St_r	=	ribbed wall Stanton number, $\dot{q}_r'' D^2/\{\dot{m}c_p(\overline{T_{wr}} - \overline{T_b})\}$
St_s	=	smooth wall Stanton number, $\dot{q}_s'' D^2/\{\dot{m}c_p(\overline{T_{ws}} - \overline{T_b})\}$
$(\overline{T_w} - \overline{T_b})$	=	average wall/bulk temperature difference in fully developed region in channel, [K]
μ	=	dynamic viscosity of air at average bulk temperature, [N·sec/m^2]
ρ	=	density of air at average bulk temperature, [kg/m^3]

Introduction

EXPERIMENTS have been conducted to study turbulent heat transfer and friction for thermally fully developed flow of air in a square channel in which two opposite walls are roughened with staggered arrays of discrete ribs. The rib array on each roughened wall is a mirror image of that on the other (that is, corresponding ribs on the two opposite walls are parallel and aligned). The ribs in consecutive rows are turned either in the same direction or in opposite directions with respect to the wall centerline (see Fig. 1). The lengths of the discrete ribs are equal to one-half of those of the corresponding full ribs and the angled discrete ribs are cut at angles equal to the rib angles-of-attack.

The rib height-to-channel hydraulic diameter ratio is 0.0625 and the rib pitch-to-height ratio is 10. The rib angles-of-attack (α) are 45 deg, 60 deg, 90 deg, +45 deg and −45 deg in alternate rows, +60 deg and −60 deg in alternate rows, +120 deg and −120 deg in alternate rows, and +135 deg and −135 deg in alternate rows. The flow Reynolds number ranges from 10,000 to 60,000. The rib-roughened channel models the internal cooling passages in modern gas turbine airfoils. The rib configurations and the Reynolds number range are typical for turbine airfoil cooling applications.

Internal cooling passages in modern gas turbine airfoils have been investigated by researchers such as Burggraf[1] and

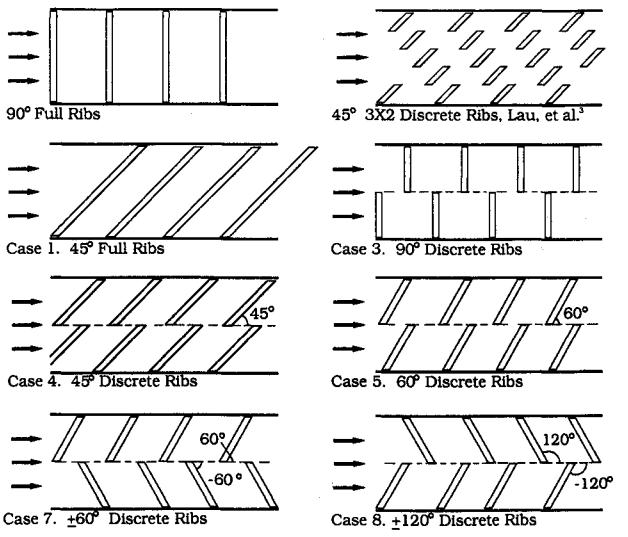

Fig. 1 Typical rib configurations.

Han et al.[2] as straight (or multipass) square (or rectangular) channels that had two opposite ribbed walls and two smooth walls. Lau et al.[3] studied the effects of replacing the angled full ribs on two opposite walls of a square channel with parallel and crossed arrays of discrete ribs on the turbulent heat transfer and friction for fully developed flow of air in the square channel. The discrete ribs were five equal-length segments of the angled full ribs cut at an angle equal to α and staggered in alternate rows of three and two ribs along oblique (parallel or crossed) lines at α with respect to the main flow. Results showed that parallel angled discrete ribs have higher thermal performance than 90 deg discrete ribs and corresponding parallel angled full ribs. Parallel discrete ribs with $\alpha = 45$ deg had the best thermal performance. Crossed arrays of angled full and discrete ribs had poor thermal performance and were not recommended.

Chyu and Natarajan[4] conducted experiments to study the heat/mass transfer from 90 deg "broken" ribs. Based on three test runs, they concluded that broken ribs enhanced less heat transfer than full ribs. The results of the present study and those of Lau et al.[3] show that their generalized conclusion is inaccurate.

Experimental Apparatus and Procedure

The open air-flow loop is similar to that used in Lau et al.[3] It consists of two centrifugal blowers connected in parallel, a by-pass valve, a gate valve, a calibrated orifice flow meter, a flow straightener, an entrance section, and the test section. The test section is the straight, uniformly heated, 7.62 cm by 7.62 cm square, aluminum channel used in Lau et al.[3]

The interior surfaces of two opposite walls of the test channel are roughened with parallel, staggered arrays of discrete ribs (see Fig. 1). The interior surfaces of the other two walls are smooth. The ribs are cut from 4.76 mm by 4.76 mm square brass bars at an angle equal to α with a slitting saw on a milling machine. They are then attached to the channel walls with silicone rubber adhesive at intervals of 4.76 cm (ten times the rib height).

Copper-constantan thermocouples are installed along the axial centerlines of the ribbed walls and the smooth walls to determine the streamwise wall temperature distributions. The first thermocouple station is located at 2.5 times the rib height from the channel entrance. Other temperature measurement stations are located at 30-rib-height intervals. Several other thermocouples along the axial centerlines of the ribbed walls and the smooth walls check the streamwise temperature variation between adjacent primary measurement stations in the thermally fully developed region. Additional thermocouples at other off-center locations on the ribbed walls check the spanwise variation of the wall temperature.

Two thermocouples measure the inlet air temperature and five thermocouples the exit air temperature. Five pressure taps are installed along the axial centerline of one of the smooth walls to determine the streamwise pressure drop.

Readers are referred to Lau et al.[3] for detailed descriptions of the test apparatus, the heat transfer, temperature, and flow rate measurements, the instrumentations, and the experimental procedure.

Data Reduction

The reduction of the experimental data follows the procedure given in Lau et al.[3] The ribbed wall and smooth wall Stanton numbers are calculated from the net heat fluxes from the ribbed walls and the smooth walls, and the average wall/bulk temperature differences. The temperature differences are the averages of the differences between the measured wall temperatures and the calculated air bulk temperatures (at the corresponding streamwise locations) over a section of the test channel where the flow is considered thermally fully developed.

The heat flux on the ribbed walls is the rate of net heat transfer from the ribbed walls to the flowing air divided by

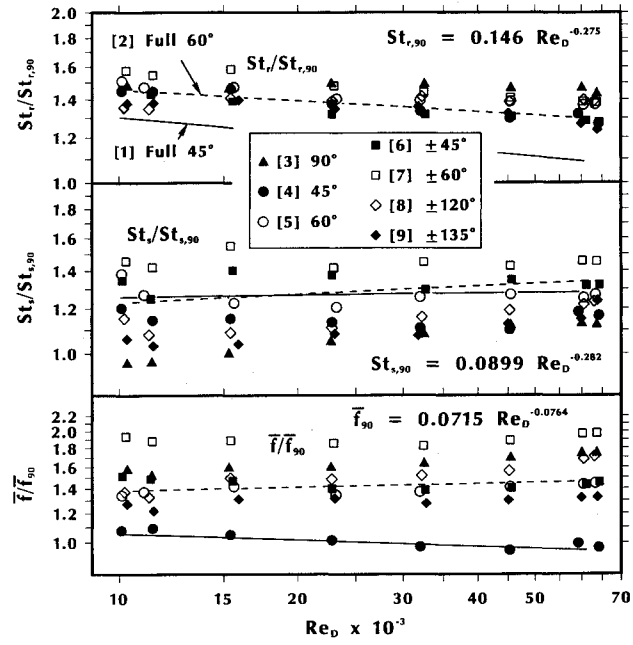

Fig. 2 $St_r/St_{r,90}$, $St_s/St_{s,90}$, and $\bar{f}/\bar{f}_{90}$ as functions of Re_D.

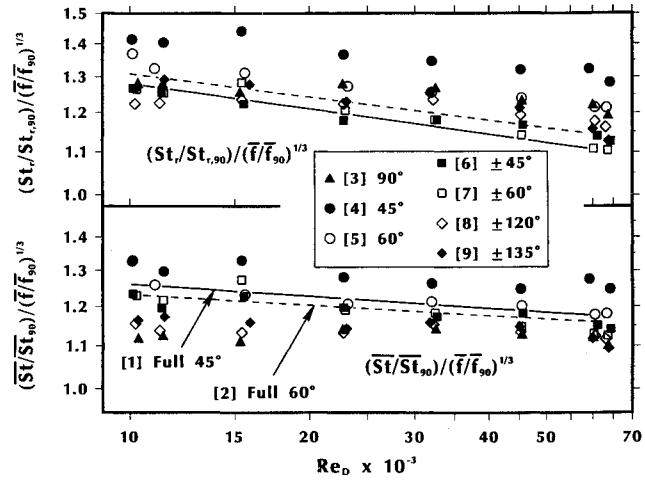

Fig. 3 Thermal performances, $[(St_r/St_{r,90})/(\bar{f}/\bar{f}_{90})^{1/3}]$ **and** $[(\overline{St}/\overline{St}_{90})/(\bar{f}/\bar{f}_{90})^{1/3}]$ **as functions of** Re_D.

the projected heat transfer area (not including the increased rib surface area). The rate of net heat transfer from each channel wall takes into account the streamwise heat conduction along the wall and the heat loss to the surroundings. The local bulk temperature is evaluated from an energy balance with the rate of net heat transfer (at each temperature measurement station) from all four walls to the air, the air mass flow rate, and the inlet bulk temperature.

The friction factor and the Stanton numbers are normalized with their corresponding values for thermally fully developed turbulent flow through a square channel that has two opposite walls roughened with 90 deg full ribs and two smooth walls: $\bar{f}_{90}$, $St_{r,90}$, $St_{s,90}$, and $\overline{St}_{90}$.

Presentation of Results

In Fig. 2, the normalized ribbed-wall Stanton number, smooth-wall Stanton number, and friction factor are plotted as functions of the Reynolds number. The values of the normalized Stanton numbers and friction factor give the improvement in heat transfer and the penalty in higher pressure drop, respectively, when 90 deg full ribs are replaced with discrete ribs. Lines representing the power functions for 45 deg and 60 deg full ribs (Cases 1 and 2, by curve fitting least-

Table 1 Coefficients and exponents of power functions for $St_r/St_{r,90}$, $\bar{f}/\bar{f}_{90}$, and $[(St_r/St_{r,90})/(\bar{f}/\bar{f}_{90})^{1/3}]$

	$St_r/St_{r,90}$		$\bar{f}/\bar{f}_{90}$		$(St_r/St_{r,90})/(\bar{f}/\bar{f}_{90})^{1/3}$	
Case/Angle	a	b	a	b	a	b
[3]/90 deg	1.53	−0.0035	0.74	0.0784	1.69	−0.0297
[4]/45 deg	2.84	−0.0716	1.94	−0.0640	2.27	−0.0503
[5]/60 deg	2.33	−0.0485	1.04	0.0286	2.30	−0.0580
[6]/±45 deg	2.63	−0.0658	1.87	−0.0257	2.14	−0.0573
[7]/±60 deg	3.16	−0.0748	1.68	0.0123	2.66	−0.0789
[8]/±120 deg	1.22	0.0129	0.47	0.1148	1.57	−0.0254
[9]/±135 deg	2.27	−0.0521	0.99	0.0265	2.28	−0.0609

squares straight lines through experimental data of Lau et al.[3]) are included for comparison.

All arrays of discrete ribs in this study enhance more heat transfer from the ribbed walls than 90 deg full ribs. Discrete ribs with α = 60 deg, ±60 deg, and ±120 deg (Cases 5, 7, and 8) generally cause higher heat transfer from the ribbed walls than discrete ribs with α = 45 deg, ±45 deg, and ±135 deg (Cases 4, 6, and 9). Among the angled discrete ribs, ±60 deg discrete ribs have the highest values of St_r. Discrete ribs with α = 90 deg (Case 3) have the highest values of St_r at large Re_D. Angled discrete ribs enhance more heat transfer from the ribbed walls than the corresponding 60 deg and 45 deg full ribs (Cases 1 and 2). The interactions between separated flows from the various edges of the discrete ribs, including those at the ends, and secondary flows are believed to cause better mixing in the flow and the generally higher heat transfer in the discrete rib cases than in the corresponding full rib cases.

Replacing the full ribs with discrete ribs in Cases 6 and 7 (α = ±45 deg and ±60 deg) also increases the heat transfer from the smooth walls. The smooth-wall Stanton numbers for other angled discrete ribs, however, are generally lower than those for full ribs with α = 60 deg and 45 deg, respectively. Discrete ribs with α = 90 deg have by far the lowest values of St_s.

Discrete ribs with α = 45 deg and 60 deg (Cases 4 and 5) cause about the same pressure drop as the 45 deg and 60 deg full ribs, respectively. Other discrete ribs cause higher pressure drop than corresponding full ribs. Among the discrete rib cases in this study, 45 deg discrete ribs (Case 4) have the lowest friction factor and ±60 deg discrete ribs (Case 7) the highest.

Figure 3 compares the thermal performances of the discrete ribs with those of the angled full ribs. The ratios $[(St_r/St_{r,90})/(\bar{f}/\bar{f}_{90})^{1/3}]$ and $[(\overline{St}/\overline{St}_{90})/(\bar{f}/\bar{f}_{90})^{1/3}]$ for all cases are plotted versus Re_D. Among the cases studied, discrete ribs with α = 45 deg (Case 4) have the best thermal performance. Their performance, however, is lower than those of parallel staggered 3 × 2 discrete-rib arrays with α = 45 deg and 60 deg (Lau et al.[3]).

Discrete ribs with α = 90 deg enhance more heat transfer from the ribbed walls (up to 50%) than 90 deg ribs but cause much higher pressure drops (up to 75%). On a per unit pumping power basis, 90 deg discrete ribs have high ribbed wall heat transfer but low overall heat transfer.

The coefficients and exponents of power functions of the Reynolds number, $a(Re_D)^b$, for $St_r/St_{r,90}$, $\bar{f}/\bar{f}_{90}$, and $[(St_r/St_{r,90})/(\bar{f}/\bar{f}_{90})^{1/3}]$ are given in Table 1. The power functions are determined by curve fitting least-squares straight lines through the experimental data.

Concluding Remarks

Discrete ribs with α = ±60 deg and 90 deg cause very high heat transfer from the ribbed walls. Discrete ribs with α = 45 deg (Case 4) have the best thermal performance. Replacing angled full ribs with these discrete ribs in cooling channels in turbine airfoils improves the thermal performance of the channels.

Acknowledgments

This research was supported by the National Science Foundation (Grant CTS-8910860).

References

[1]Burggraf, F., "Experimental Heat Transfer and Pressure Drop with Two-Dimensional Turbulence Promoter Applied to Two Opposite Walls of a Square Tube," *Augmentation of Convective Heat and Mass Transfer*, edited by A. E. Bergles and R. L. Webb, American Society of Mechanical Engineers, New York, 1970, pp. 70–79.

[2]Han, J. C., Park, J. S., and Lei, C. K., "Heat Transfer Enhancement in Channels with Turbulence Promoters," *ASME Journal of Engineering for Gas Turbines and Power*, Vol. 107, July 1985, pp. 629–635.

[3]Lau, S. C., McMillin, R. D., and Han, J. C., "Heat Transfer Characteristics of Turbulent Flow in a Square Channel with Angled Discrete Ribs," ASME Paper 90-GT-254, 1990, and *ASME Journal of Turbomachinery*, Vol. 113, July 1991, pp. 367–374.

[4]Chyu, M. K., and Natarajan, V., "Local Heat Transfer on a Flat Surface Roughened with Broken Ribs," presented at the 1989 ASME Winter Annual Meeting, San Francisco, CA, ASME HTD-Vol. 120, 1989, pp. 25–31.

Practical Method for Calculating Radiation Incident upon a Panel in Orbit

Masao Furukawa*
National Space Development Agency, Tsukuba, Ibaragi 305, Japan

Introduction

DETERMINATION of external radiation incident upon flat plates or area elements is indispensable for thermal design practice of a satellite for which temperatures will passively be controlled. In determining radiant transfer from the sun or the earth to a specified surface, one needs a precise knowledge of angle factors showing the rates of radiation directly intercepted by the surface. Such view factors was first considered by Katz[1] and then by Hrycak,[2] and some of them were calculated by Ballinger et al.[3] Cunningham[4,5] presented analytical expressions of earth-reflected solar radiation input to spherical satellites. Also given by Cunningham[6–8] are expressions for calculating thermal radiation from the earth

Received May 18, 1990; revision received Aug. 7, 1990; accepted for publication Aug. 16, 1990.

*Senior Engineer, System Engineering Division, Tsukuba Space Center, 2-1-1, Sengen.